

CHAPTER 1

INTRODUCTION

Surface turbulent heat fluxes, driven by the mean wind speed, air/sea temperature difference, and vertical moisture gradients, are an important mechanism for transporting heat from the ocean to the atmosphere. Modulations in the large scale atmospheric circulation and sea surface temperature patterns induce changes in latent and sensible heat fluxes over large spatial scales. Therefore, the surface heat fluxes are indicators of changes in the climate system, with links to anomalous mid-latitude storm tracks and precipitation patterns over the North Atlantic and neighboring regions. This study examines the spatial and temporal variability of the surface turbulent heat fluxes over the North Atlantic (10°S-62°N) using the new objectively produced FSU3 monthly 1°x 1° gridded wind and surface flux product for 1978-2003.

Several studies (Zhao and McBean 1986; Cayan 1992; Alexander and Scott 1997) have examined the basin wide variability of the surface heat fluxes over the North Pacific and Atlantic Oceans. The studies concluded that the latent and sensible heat fluxes respond to changes in the low level atmospheric circulation patterns, thus are closely linked to the dominant atmospheric circulation modes, e.g., the North Atlantic Oscillation (NAO) and Pacific-North American (PNA) pattern (Cayan 1992; Alexander and Scott 1997). Anomalous fluxes have been shown to be organized over regions of atypical wind speed and meridional flow. Cayan (1992) found that for the mid and upper latitude regions of the North Atlantic the wind direction explained approximately 20% to 45% of the flux variability, whereas in the tropics the wind direction had little influence on the monthly variations due to the small horizontal gradients of temperature and moisture, and the constancy of the trade winds.

This analysis focuses on a low frequency (basin wide) mode of variability that is hypothesized to be linked to changes in the large scale circulation patterns (meridional pressure gradients) possibly associated with the Atlantic Multidecadal Oscillation (AMO; Schlesinger and Ramankutty 1994; Kerr 2000). The latent and sensible heat fluxes show a transition from predominantly positive to negative anomalies around 1998. The interdecadal variability of the surface turbulent heat fluxes appears to be primarily forced by changes in the wind speed.

The input data, bias corrections, and quality control procedures are described in chapter 2. Chapter 3 discusses the objective method used to grid the in situ ship and buoy observations. A description of the AMO, NAO, and El Nino-Southern Oscillation (ENSO) along with the influence each have on the turbulent heat fluxes and associated variables is presented in chapter 4. The results are presented in chapter 5. For example, clear dissimilarities are evident between the sensible and latent fluxes during 1982-1997 and 1998-2003. The largest significant changes occur over the tropics, Gulf Stream, and higher latitude regions of the North Atlantic.

CHAPTER 2

DATA

In situ ship and buoy (moored and drifting) observations are used to objectively produce monthly mean fields of wind stress (τ), latent heat flux (E), sensible heat flux (H), pseudostress (Ψ), scalar wind speed (w), specific humidity (q), and air temperature (AT). Fields prior to and including 1997 are generated using the International Comprehensive Ocean-Atmosphere Data Set (ICOADS; Woodruff et al. 1987; Worley et al. 2005), and data from the National Climatic Data Center (technical document Marine Surface Observations TD-1129; NCDC 2003) are used for the subsequent years.

The ICOADS dataset is constructed of historical marine data obtained from a multitude of sources, e.g., merchant ships, fishing vessels, buoys, and foreign meteorological services, that extend back to 1854 (Woodruff et al. 1987). Due to the large amount of processing the ICOADS dataset is updated approximately every 3 to 8 years. TD-1129, updated annually, is a subset of ICOADS and contains real time and delayed mode oceanic reports collected by NCDC since 1982 via the Global Telecommunication System (GTS). The inclusion of TD-1129 data into ICOADS allows duplicate observations to enter the dataset; thus a detailed quality control procedure (Woodruff et al. 1998) is implemented to eliminate matching reports. The quality control procedure also identifies many erroneous observations and the type of observing platform associated with each report (when available). Metadata from ICOADS and TD-1129 are used in bias corrections (see section 2.1).

The observations are binned on a 1° by 1° grid and a monthly mean is computed for each variable in each grid box with data. Buoy reports are daily averaged into a superobservation prior to determining the number of observations per month, due to a

lack of independence of hourly data. Initially, the wind stress, sensible and latent heat fluxes are computed (Bourassa et al. 1999) from individual observation records that contain wind speed and direction, air temperature, specific humidity, and sea surface temperature. The surface fluxes are also averaged monthly on the same 1° by 1° grid.

The National Meteorological Center's (NMC) blended sea surface temperature analysis (referred to as Reynolds SSTs hereafter; Reynolds 1988) is used to compute the sensible heat flux during the variational method. The use of the blended product is due to the fact that bias corrections for ship based sea surface temperatures are not well understood and vary greatly on a ship to ship basis. The blended analysis merged the NMC's in situ sea surface temperature product with their satellite analysis. The blending procedure utilized the in situ analysis for regions of high density in situ observations whereas the satellite analysis was used for regions containing an insufficient amount of in situ data. Reynolds (1988) showed that the satellite analysis has little influence on the blended fields from 60°N to the equator in the Atlantic Ocean due to the large quantity of in situ observations. For this region the calculated fluxes are similar to those calculated with the Reynolds SSTs.

2.1 Bias Corrections

Prior to the calculation of the wind stress and surface heat fluxes, known systematic errors are removed from the data. Air temperature measurements from Voluntary Observing Ships (VOS) and buoys are known to contain systematic biases associated with the heating of the ship's infrastructure and instruments by solar radiation (Berry et al. 2004). In order to compute surface fluxes to within 10 Wm^{-2} the air temperature should be measured to an accuracy of $\pm 0.2^\circ\text{C}$ (Taylor et al. 2000). The error in air temperature measurements associated with solar heating can be greater than 0.2°C and larger than the air/sea temperature difference, thus resulting in inaccurate surface flux calculations (Berry et al. 2004). Since the sensible heat flux is directly dependent on the air/sea temperature difference, the air temperature bias can produce an unrealistic transfer of heat. In addition, the momentum and heat fluxes are also dependent on the atmospheric stability via the transfer coefficients; therefore unrealistic stable or near-neutral conditions caused by the air temperature error can result in a reduced magnitude

of the surface fluxes. In order to remove the radiative heating errors from the VOS observations a heat budget model developed by Berry et al. (2004) was applied to the monthly averaged data using 30 Wm^{-2} to represent the monthly mean solar heating.

The surface fluxes are regulated by the interaction of the sea surface and overlying atmospheric conditions, thus the Reynolds SSTs must be corrected to represent a skin temperature. The skin temperature is sensitive to local changes in heat and momentum fluxes; therefore the bulk minus skin temperature difference is highly variable on short time scales and latitudinal dependent (Donlon and Robinson 1997). Overall, Donlon and Robinson (1997) calculated a mean bulk minus skin temperature difference of $0.35 \text{ K} \pm 0.35 \text{ K}$. As a result, a value of 0.3°C is added to the monthly mean Reynolds SSTs.

Visually estimated (Beaufort) winds are converted to a 10 m wind speed value using the Lindau (1995) “Beaufort equivalent scale”. The anemometer wind speed observations are height adjusted to a standard height of 10 m using a surface flux model (Bourassa et al. 1999). Ship anemometer observations are presumed to correspond to a 20 m reference height whereas buoy anemometer heights are known. The assumption of a constant reference height introduces errors and a trend due to the increasing measurement heights with time. However, the detailed metadata required to accurately height adjust the ship wind speed observations are only available from the mid 1990s. Using the limited metadata would add a substantial discontinuity to the dataset.

2.2 Quality Control

Three quality control procedures are implemented to remove erroneous and non-representative observations from the data sets. The first quality control procedure is applied to the individual observations; whereas the remaining two are implemented on the monthly mean gridded fields. First, the individual observations are compared to climatological values. A monthly mean and standard deviation are computed using the daSilva climatology (daSilva et al. 1994). Data that fall outside 3.5 standard deviations from the monthly mean are eliminated. In addition, a minimum standard deviation for each variable is also imposed due to the limited variability of the deSilva climatology in certain regions of the globe (Bourassa et al. 2005). This comparison removes very few

observations, most of which are grossly inconsistent with nearby observations. For the 26 years of data that have been examined, no clusters of data have been removed; indicating that this comparison has not caused excessive trimming.

The second quality control procedure termed “auto-flag” is applied to the monthly mean gridded ship observations. This process flags and removes grid points that differ too much from adjacent points. The auto-flag routine computes differences between nearest neighboring grid boxes for each scalar variable: air temperature, sea surface temperature, specific humidity, wind speed, and u and v pseudostress components. Differences in adjacent grid boxes are (on average) larger in regions with greater natural variability. Local monthly variabilities are estimated as standard deviations of a five year average (1999-2003) of 6 hourly European Centre for Medium-Range Weather Forecasts (ECMWF) reanalyses. The absolute value of each difference is divided by the square root of the standard deviation to account for regional variability. Subjective analysis of the fields indicated that this procedure was quite effective in removing regional biases in the quality control technique. These adjusted differences are ordered by magnitude and the grid boxes associated with the top three percent of the greatest differences receive flags. A datum is removed (set equal to a designated missing value) based on the total number of flags a particular grid box receives for that variable. Air temperature, sea surface temperature, and specific humidity are removed (on a variable by variable basis) if a grid box contains five or more flags for that variable. Wind speed data are removed if a grid box contains four or more flags. Lastly, if in three or more of the scalar variables an individual grid box was set to missing, then the grid cell and associated data are completely eliminated from that particular month’s data set. Tests were again made to verify that this approach did not remove clusters of data. The FSU3 fluxes are the first version of the FSU winds to employ the auto-flag technique. Doing so has reduced the human component of processing time by approximately a factor of ten.

The third quality control procedure utilizes a tool developed to display the monthly mean gridded ship and buoy observations. An analyst visually inspects the monthly in situ fields and subjectively removes suspect data that were not eliminated by the preceding quality control methods. The edits are made in data sparse regions, where

the auto-flag procedure cannot effectively be applied. Very few data are removed in this step, which is the most time intensive as it is not automated.

CHAPTER 3

OBJECTIVE METHOD

3.1 Variational Method

A variational method is utilized to objectively grid in situ ship and buoy observations. A cost function based on weighted constraints is minimized via a conjugate-gradient minimization scheme (Shanno and Phua 1980). The constraints help to maximize the similarity of the solution fields to the observations and minimize unrealistic spatial features. Three constraints are applied to the vector variables: a misfit to observations, a Laplacian smoothing term, and a misfit of the curl. The first two constraints are applied to scalar variables. The smoothing and curl terms, applied to differences between the solution field and background field, relate information at an individual grid point to neighboring grid points to ensure spatial consistency (Pegion et al. 2000, Bourassa et al. 2005). Each constraint is multiplied by a weight that is determined using cross validation (Wahba and Wendelberger 1980) prior to the minimization of the functional.

The cost function implemented is

$$\begin{aligned}
 f = & \sum_{i,j}^{I,J} \{ \beta_{\Psi_{o1}} \sigma_{\Psi_{o1}}^{-2} [(\Psi_x - \Psi_{x_{o1}})^2 - (\Psi_y - \Psi_{y_{o1}})^2] + \beta_{\Psi_{o2}} \sigma_{\Psi_{o2}}^{-2} [(\Psi_x - \Psi_{x_{o2}})^2 - (\Psi_y - \Psi_{y_{o2}})^2] + \\
 & \beta_{\Psi_{o3}} \sigma_{\Psi_{o3}}^{-2} [(\Psi_x - \Psi_{x_{o3}})^2 - (\Psi_y - \Psi_{y_{o3}})^2] + \beta_{\Psi_{Lap}} L^4 [\nabla^2 (\Psi_x - \Psi_{bg})^2] + \\
 & \beta_{\Psi_{Lap}} L^4 [\nabla^2 (\Psi_y - \Psi_{bg})^2] + \beta_{\Psi_{curl}} L^2 [\hat{k} \bullet \nabla \times (\Psi - \Psi_{bg})^2] + \beta_{AT_{o1}} \sigma_{AT_{o1}}^{-2} (AT - AT_{o1})^2 + \\
 & \beta_{AT_{o2}} \sigma_{AT_{o2}}^{-2} (AT - AT_{o2})^2 + \beta_{AT_{Lap}} L^4 [\nabla^2 (AT - AT_{bg})]^2 + \beta_{q_{o1}} \sigma_{q_{o1}}^{-2} (\ln(q) - \ln(q)_{o1})^2 + \\
 & \beta_{q_{o2}} \sigma_{q_{o2}}^{-2} (\ln(q) - \ln(q)_{o2})^2 + \beta_{q_{Lap}} L^4 [\nabla^2 (\ln(q) - \ln(q)_{bg})]^2 + \beta_{w_{o1}} \sigma_{w_{o1}}^{-2} (\ln(w) - \ln(w)_{o1})^2 + \\
 & \beta_{w_{o2}} \sigma_{w_{o2}}^{-2} (\ln(w) - \ln(w)_{o2})^2 + \beta_{w_{Lap}} L^4 [\nabla^2 (\ln(w) - \ln(w)_{bg})]^2 +
 \end{aligned}$$

$$\begin{aligned}
& \beta_{\tau_{o1}} \sigma_{\tau_{o1}}^{-2} [(\tau_x - \tau_{x_{o1}})^2 - (\tau_y - \tau_{y_{o1}})^2] + \beta_{\tau_{Lap}} L^4 [\nabla^2 (\tau_x - \tau_{bg})]^2 + \beta_{\tau_{Lap}} L^4 [\nabla^2 (\tau_y - \tau_{bg})]^2 + \\
& \beta_{\tau_{curl}} L^2 [\hat{k} \cdot \nabla \times (\boldsymbol{\tau} - \boldsymbol{\tau}_{bg})]^2 + \beta_{H_{o1}} \sigma_{H_{o1}}^{-2} (H - H_{o1})^2 + \\
& \beta_{H_{Lap}} L^4 [\nabla^2 (H - H_{bg})]^2 + \beta_{E_{o1}} \sigma_{E_{o1}}^{-2} (E - E_{o1})^2 + \beta_{E_{Lap}} L^4 [\nabla^2 (E - E_{bg})]^2, \tag{1}
\end{aligned}$$

where i and j are indices for the longitude and latitude and have been dropped from the terms in the functional, β represents the weights determined by cross validation (Table 1), the unsubscripted variables are the solution field, the ‘ o ’ subscript represents observations (‘ $o1$ ’ for ships, ‘ $o2$ ’ for moored buoys, and ‘ $o3$ ’ for drifting buoys), ‘ bg ’ indicates the background field, L is a grid-spacing dependent non-dimensional scale that make the weights approximately independent of grid spacing, and σ is an estimate of local variability (uncertainty squared). The local uncertainty in the observations is estimated from the mean monthly variability based on six-hourly observations in the NCEP/NCAR reanalysis (Kalnay et al. 1996):

$$\sigma^2 = \frac{\sigma_{NCEP}^2}{n}, \tag{2}$$

where n is the number of ship observations per month. The uncertainties for the Laplacian and curl terms are treated as a global average and combined with the weights.

Table 1. Objectively determined weights.

| Term | Weight | Term | Weight |
|-----------------------|---------------|-----------------------|---------------|
| $\beta_{\psi_{o1}}$ | 1.0 | β_{wo1} | 1.0 |
| $\beta_{\psi_{o2}}$ | 20.0 | β_{wo2} | 10.0 |
| $\beta_{\psi_{o3}}$ | 0.1 | β_{wLap} | 120.0 |
| $\beta_{\psi_{Lap}}$ | 0.6 | $\beta_{\tau_{o1}}$ | 0.0378 |
| $\beta_{\psi_{curl}}$ | 1.0 | $\beta_{\tau_{Lap}}$ | 1.24 |
| β_{ATo1} | 1.0 | $\beta_{\tau_{curl}}$ | 1.20 |
| β_{ATo2} | 0.01 | β_{Ho1} | 0.92 |
| β_{ATLap} | 1400.0 | β_{HLap} | 17.3 |
| β_{qo1} | 0.008 | β_{Eo1} | 5.27 |
| β_{qo2} | 0.01 | β_{ELap} | 117.8 |
| β_{qLap} | 6.00 | | |

3.2 Background Field

The background fields are excessively smooth monthly fields derived from the observations from the month being examined. The use of individual monthly averages was found to be more effective than using a long-term climatology (Bourassa et al. 2005). A Gaussian weighted spatial average is applied to the in situ monthly fields to determine the values at each grid point. The weight is a function of the distance, measured in units of grid cells, away from the grid point of interest. The spatial averaging is dependent on the total number of observations. A minimum of 100 observations is desired for winds, temperatures, and humidities, while a minimum of 15 is required. However, for specific humidity and air temperature 100 observations are required near the equator and gradually dropping to 25 at approximately $\pm 38^\circ$. In areas containing an inadequate number of observations the search radius is increased by one grid cell until a sufficient number is obtained or a maximum search area is exceeded. The search area in the open ocean is bounded by a lower and upper limit, 5 and 11 grid cells respectively. In the few regions where the minimum observation requirement is not satisfied the background field is determined by averaging neighboring values of the background field in a creeping fill (Kara et al. 2005). A “line of sight” constraint prohibits data associated with considerably differing regimes from being included in the Gaussian spatial averaging procedure (Bourassa et al. 2005). This restriction permits only observations that have a line of sight free of land to be utilized in determining a value in the background field.

3.3 Flux Calculations

The wind stress, sensible heat flux, and latent heat flux are calculated from the monthly averaged variables via the bulk flux formulas:

$$\tau = \rho C_D \Psi, \quad (3)$$

$$H = \rho c_p C_H (SST - AT) w, \quad (4)$$

$$E = \rho L_v C_E (q_{sfc} - q) w, \quad (5)$$

where ρ is the density of moist air, c_p is the specific heat of air, L_v is the latent heat of vaporization, C_D is the drag coefficient, C_H is the heat transfer coefficient, C_E is the moisture transfer coefficient, SST is the mean sea surface temperature, AT is the mean air temperature, q_{sfc} is the mean specific humidity near the surface, q is the mean specific humidity, w is the mean scalar wind speed, and Ψ is the vector pseudostress. The zonal (Ψ_x) and meridional (Ψ_y) components of the pseudostress are defined as:

$$\Psi_x = uw, \quad (6)$$

$$\Psi_y = vw, \quad (7)$$

where u and v represent the mean zonal and meridional components of the wind vector.

CHAPTER 4

NORTH ATLANTIC MODES OF CLIMATE VARIABILITY

This section discusses three climate modes that influence the low frequency variability of the latent and sensible heat fluxes over the North Atlantic Ocean. The AMO, NAO, and ENSO all influence the variables that force the turbulent heat fluxes via changes in the large scale circulation or sea surface temperature patterns. However, each aforementioned climate mode varies on differing time scales with distinct action centers. Understanding the spatial and temporal variability associated with each climate signal will help to interpret the longer time scale changes in the latent and sensible heat fluxes presented in chapter 5.

4.1 Atlantic Multidecadal Oscillation

Schlesinger and Ramankutty (1994) identified a North Atlantic surface temperature oscillation, using global mean temperature records, with a period of 65-70 years. This oscillation, later termed the Atlantic Multidecadal Oscillation (Kerr 2000) is described as the leading mode of low-frequency sea surface temperature variability throughout the North Atlantic and thought to be forced by fluctuations in the thermohaline circulation (Delworth and Mann 2000). The AMO is characterized by sea surface temperature anomalies of the same sign over the entire North Atlantic with the largest values located east of Newfoundland (Sutton and Hodson 2005). Warm phases are associated with the time periods of 1860-1880 and 1930-1960 with cool phases during 1905-1925 and 1970-1990. The AMO appears to have transitioned back to a warm phase during the mid 1990s (Grey et al. 2004).

Past studies have connected the AMO to anomalous precipitation patterns over the North Atlantic and neighboring areas as well as to North Atlantic hurricane activity.

The warm phase is associated with decreased rainfall over the central United States and northern Mexico and enhanced precipitation over the northeast United States, Florida, and the tropical North Atlantic extending from the Caribbean into the Sahel region of Africa (Enfield et al. 2001; Goldenberg et al. 2001; Sutton and Hodson 2005). The warm phase of the AMO is also associated with a greater amount of Caribbean tropical cyclones and North Atlantic major hurricanes resulting from increased sea surface temperatures and decreased vertical shear (Goldenberg et al. 2001).

4.2 North Atlantic Oscillation

The NAO, first discussed by Walker and Bliss (1932), is a large scale fluctuation of atmospheric mass with the main action centers located near the Icelandic Low and Azores High. The positive phase of the NAO is associated with anomalously low surface-pressure over the subarctic regions and higher surface-pressure across the subtropical north Atlantic. The opposite scenario is true for the negative phase. Consequently, the westerlies and northeast trade winds across the North Atlantic are intensified (weakened) during the positive (negative) phase. The westerlies are over 8 ms^{-1} stronger during positive NAO winters (Hurrell 1995). In addition to the modulation of the zonal winds, anomalous meridional flow is also observed. During the positive phase, anomalous northerly flow occurs over western Greenland, the Canadian Arctic, and the Mediterranean with anomalous southerly flow over the eastern United States.

The NAO controls much of the climate variability over the North Atlantic and surrounding continents during the boreal winter (Hurrell and Dickson 2004). Temporally, the NAO fluctuates on multiple time scales thus influencing both the short (intraseasonal and interannual) and longer (interdecadal) term variability. Past studies have linked the NAO to changes in North Atlantic winter storm tracks and intensity (Rogers 1990, 1997; Hurrell and van Loon 1997; Serreze et al. 1997; Deser et al. 2000), precipitation patterns (Lamb and Pepler 1987; Hurrell 1995), air temperature and SST patterns (van Loon and Rogers 1978; Hurrell and Dickson 2004), and surface turbulent heat fluxes (Cayan 1992; Alexander and Scott 1997).

Cayan (1992) showed that the surface heat flux anomalies coincide with regions of anomalous wind speed and meridional temperature/moisture advection. During

positive NAO winters, positive latent and sensible heat flux anomalies are located east of Labrador, south of Greenland, off the northern coast of Africa, and across the tropical North Atlantic (associated with enhanced wind speed and cold dry air advection). Negative anomalies occur offshore of the United States, near Great Britain and Scandinavia (associated with relatively warm moist air advection). Cayan (1992) found that the monthly averaged latent and sensible heat fluxes poleward of 40°N were approximately 30 Wm⁻² to 90 Wm⁻² greater during positive NAO winters. Over the midlatitude North Atlantic (south of 40°N) the heat fluxes are greater during negative NAO winters with latent heat flux changes comparable in magnitude to those found north of 40°N. The tropics are in phase with the high latitude regions, but with maximum latent heat flux changes of roughly 30 Wm⁻².

4.3 El Nino-Southern Oscillation

The Southern Oscillation is a large scale fluctuation of surface pressure between the eastern and western tropical Pacific. The El Nino (warm) phase is characterized by high surface pressure over the western and low surface pressure over the southeastern tropical Pacific, with anomalously warm surface waters, weakened trade winds, and enhanced precipitation across the central/eastern basin (Philander 1990). The La Nina (cold) phase is associated with high surface pressure over the eastern and low surface pressure over the western tropical Pacific. The trade winds are strengthened, while anomalously low SSTs and rainfall occur over the eastern tropical Pacific. In addition to influencing the SST and wind fields over the tropical Indian and Pacific Oceans, ENSO is also shown to influence the SST and wind patterns over the tropical North Atlantic (Curtis and Hastenrath 1995).

Warm phases have been linked to anomalously warm surface water across the tropical North Atlantic and diminished northeast trade winds; whereas cold phases result in opposite patterns. The warm SST anomalies over the central/eastern Pacific, during a warm ENSO event, force an almost simultaneous change in the zonal sea level pressure patterns (Giannini et al. 2001). Lower sea level pressure is observed over the central/eastern Pacific with higher surface pressure over the equatorial Atlantic. Consequently, the meridional sea level pressure gradient in both hemispheres of the

Atlantic is reduced and the trade winds are weakened. As a result, the tropical North Atlantic tends to become anomalously warm following a warm ENSO event with a lag of roughly one season between the maximum anomalous SSTs in the tropical Pacific and equatorial North Atlantic (Giannini et al. 2001). According to Curtis and Hastenrath (1995), the warming of the tropical North Atlantic is the result of many factors with the response of the latent heat flux to the diminished trade winds being of primary importance. The latent heat flux responds to changes in wind speed and thus fluctuates in phase with the magnitude of the trade winds. During a warm ENSO event the weakened trade winds across the tropical North Atlantic result in decreased latent heat fluxes that ultimately contribute to the warmer SSTs.

CHAPTER 5

RESULTS

5.1 Empirical Orthogonal Function Analysis

The leading mode of the latent heat flux (~26% of the total variance) depicts a basin-wide spatial pattern where much of the North Atlantic is dominated by positive loadings (Figure 1a). The main action centers are located over the tropical North Atlantic (centered along 15°N), the Caribbean Sea, the Gulf Stream, and regions north of 50°N. Large negative loadings are limited to a region along the northern flank of the Gulf Stream. Temporally, the spatial pattern exhibits interdecadal variability (Figure 1b) with predominantly positive amplitude values throughout 1982-1997 and negative values during the subsequent years. Collectively, mode 1 illustrates a situation where the majority of the North Atlantic is dominated by positive latent heat flux anomalies during 1982-1997 with a shift to negative anomalies around 1998. The opposite is true for the New England coast region where the anomalies transition to positive values after 1997.

The leading mode of the sensible heat flux (~21% of the total variance) shows similar spatial and temporal patterns (Figure 2) to that of the latent heat flux. The main positive action centers are located over regions poleward of 45°N; however positive loadings are shown throughout the tropical and central portions of the North Atlantic. Negative loadings are limited to areas along the east coast of North America and the Scandinavian region. Figure 2b also shows evidence of longer time scale variability, with primarily positive amplitude values during 1982-1997 and negative values thereafter. Thus, mode 1 shows a change in sign of the sensible heat flux anomalies around 1998.

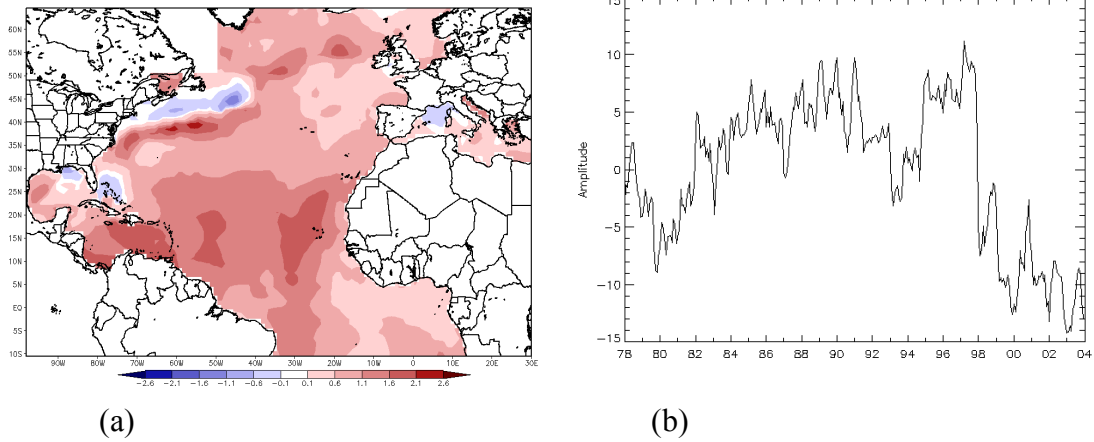


Figure 1. Empirical orthogonal function (EOF) analysis performed on monthly latent heat flux anomalies for the time period 1978-2003. Anomalies filtered (temporally) prior to the EOF analysis. (a) Spatial pattern associated with the leading mode of variability. (b) Principle component time series for the leading mode. The year labels mark January for each year.

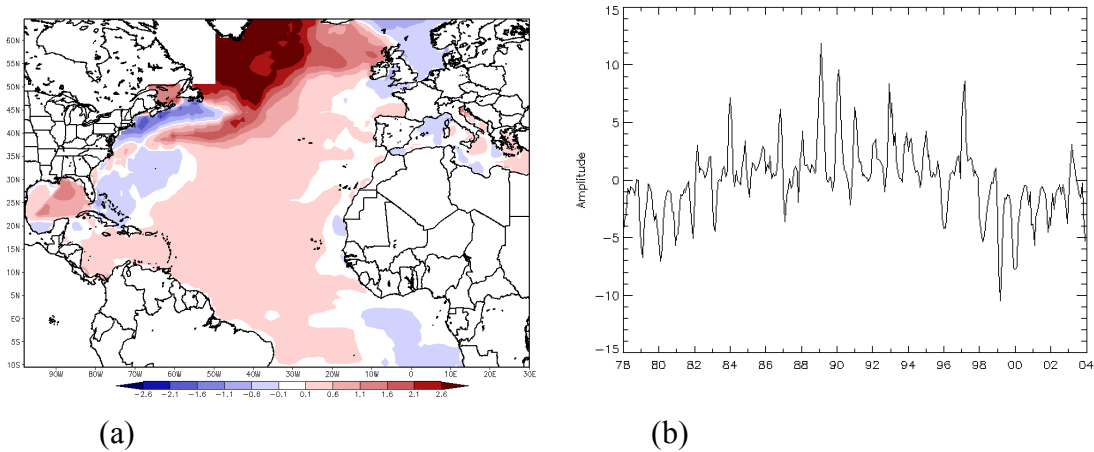


Figure 2. Same as figure 1 except for the sensible heat flux.

5.2 Interdecadal Comparison

Zonal averages help explain the basin wide interdecadal variability depicted by the EOF analysis. Zonal averages of the surface turbulent heat fluxes and associated variables are computed for each year and overall time period (1978-2003) and displayed as a function of latitude (Figure 3). A clear distinction is evident (Figure 3a and 3b)

between the latent and sensible heat fluxes for 1982-1997 (red lines) and 1998-2003 (blue lines) from roughly the equator to 40°N. Larger values are depicted for the earlier time period, coinciding with a cool phase of the AMO. The dissimilarity is less evident, over areas south of the equator and north of 40°N. These regions have relatively large uncertainty. North of 40°N there is increased natural variability and similar or reduced sampling. South of the equator there is greatly reduced sampling. The 1978-1981 time period (not shown) exhibits similar characteristics, especially over the tropical North Atlantic, to that of 1998-2003.

The wind speed (Figure 3c), similar to the latent and sensible heat fluxes, exhibits a fairly clear distinction between the two time periods, with greater values during 1982-1997. The differences in wind speed correspond to the changes illustrated in figures 3a and 3b, stronger (weaker) winds tend to intensify (diminish) the turbulent heat fluxes. The specific humidity and air/sea temperature differences (Figure 3d and 3e respectively) do not show the clear separation between the two time periods. Certain regions, between roughly 10°N and 20°N, do show some evidence for larger differences during 1982-1997, but over the majority of the basin the two time periods are generally indistinguishable. The zonal averages for the *SST* and air temperature (not shown) change in parallel, meaning that the air/sea temperature differences remain fairly constant. This would not be true over shorter time scales near land where cold (dry) air outbreaks can dramatically alter the air/sea temperature and moisture differences, resulting in large latent and sensible heat fluxes. However, it is expected in the open ocean on monthly time scales due to the lack of strong advection. Based on the zonal averages, the wind speed appears to be the key variable that is forcing the AMO-related changes in the turbulent heat fluxes.

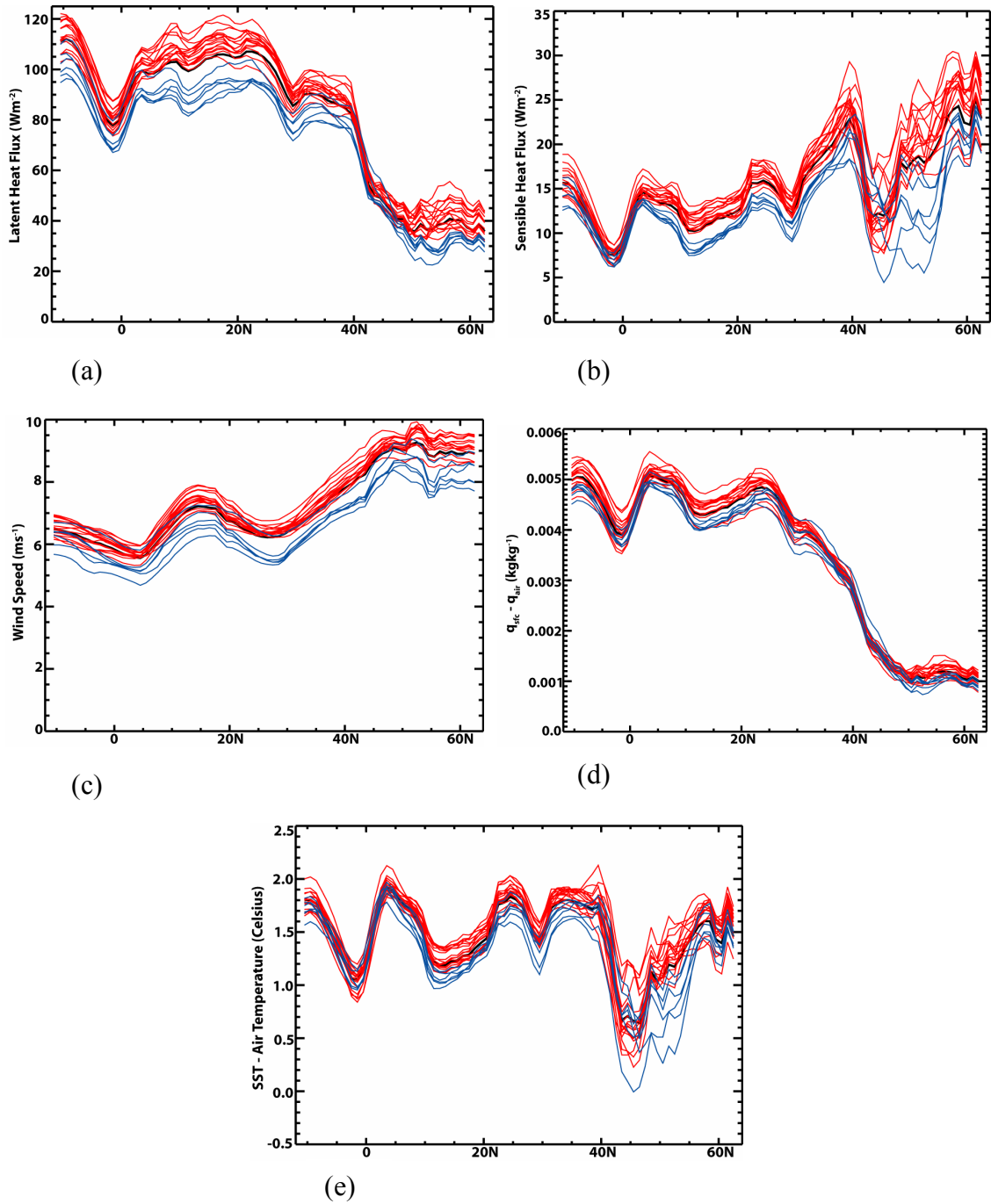


Figure 3. Zonal averages (10.5°S - 62.5°N) of the turbulent heat fluxes and associated variables for 1978-2003. Black line signifies the overall mean (1978-2003). Red lines represent yearly averages for the 1982-1997 time period. Blue lines represent yearly averages for 1982-2003. (a) Latent heat flux (Wm^{-2}). (b) Sensible heat flux (Wm^{-2}). (c) Wind speed (ms^{-1}). (d) Specific humidity differences (kgkg^{-1}). (e) Air/sea temperature difference ($^{\circ}\text{C}$).

Figure 4 quantifies the dissimilarities and statistical confidence between the 1982-1997 and 1998-2003 time periods. The latent heat flux differences (Figure 4a) are predominantly positive over the entire North Atlantic, implying larger values for 1982-1997. The largest statistically significant differences, ranging from 15 to greater than 25 Wm^{-2} , are located over the tropics, Caribbean Sea, Gulf Stream, and regions poleward of 50°N. The sensible heat flux differences (Figure 4b) show similar spatial features to that of the latent heat flux, with positive values dominating the majority of the North Atlantic basin. However, more pronounced negative values are located along the New England coast, with magnitudes exceeding 14 Wm^{-2} . Differences across the tropics, although much smaller, are still statistically significant.

The largest AMO-related wind speed differences (Figure 4c) appear to be organized around the periphery of the subtropical high, with the greatest values ($> 1.4 \text{ ms}^{-1}$) located off the northwest coast of Africa, northeast coast of the United States, over the western Gulf of Mexico, and west of the British Isles. The location of the largest differences coincides with major shipping tracks, thus it is a concern that the changes in wind speed are due to changes in observational practices rather than physical processes. The fact that greater wind speeds occur during the earlier time period contradicts the idea that the dissimilarities are due to increasing measurements heights with time. In addition, similar spatial features to those shown in figure 4c were found using the Special Sensor Microwave/Imager (SSM/I) derived monthly averaged wind speeds to compare the pre and post 1998 time period. Figure 5 depicts greater values for the pre 1998 with the largest differences located over the tropics centered along 15°N and mid-latitude regions of the North Atlantic. As a result, figure 4c and 5 suggest that the differences are related to physical processes, e.g., changes in the meridional pressure gradient, rather than data processing issues.

Figure 6b shows an enhancement of the northeast trade winds and westerlies during 1982-1997. Conversely, Figure 6c shows anomalies that imply a weakening of the large scale circulation patterns during 1998-2003. If the changes in low level circulation extend sufficiently upward, the meridional transport of energy by the mean circulation would be influenced by the phase of the AMO. When the transport due to the

mean flow is decreased it is possible that transients (e.g., tropical cyclones) or the thermohaline circulation play an increased role in transporting energy poleward.

The moisture and air/sea temperature differences (Figure 4d and 4e respectively) have similar spatial features. The largest positive values are located over the tropics and higher latitude regions with magnitudes ranging from 0.0003-0.0007 kgkg^{-1} for the humidity and 0.2 to greater than 1.0 $^{\circ}\text{C}$ for the air/sea temperature differences. Negative differences are located north of the Gulf Stream for both variables; however figure 4d also shows negative values over the Gulf of Mexico for the humidity differences with the greatest magnitude exceeding 0.9 gkg^{-1} .

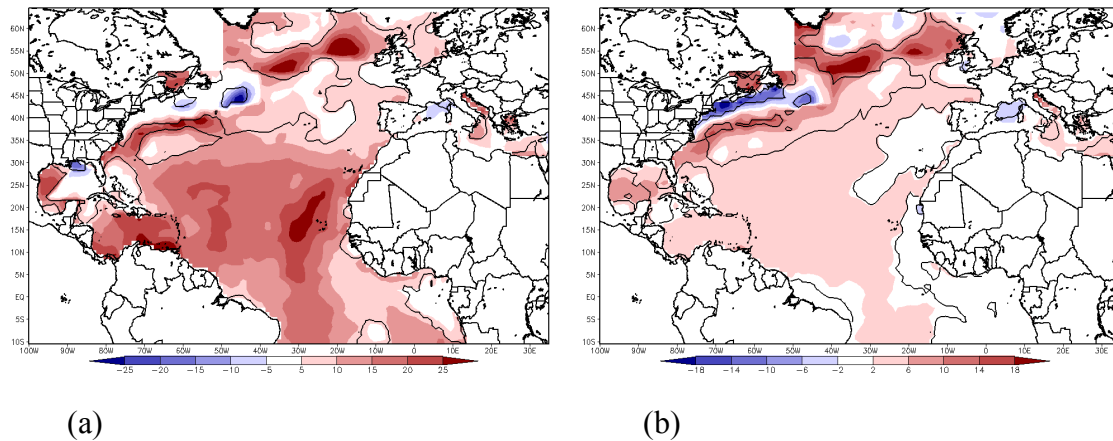


Figure 4. 1982-1997 overall mean minus 1998-2003. (a) Latent heat flux (Wm^{-2}). (b) Sensible heat flux (Wm^{-2}). (c) Wind speed (ms^{-1}). (d) Specific humidity difference (kgkg^{-1}). (e) Air/sea temperature difference ($^{\circ}\text{C}$). Solid black line represents where the difference exceeds the 95% confidence limit via a two-tailed t test.

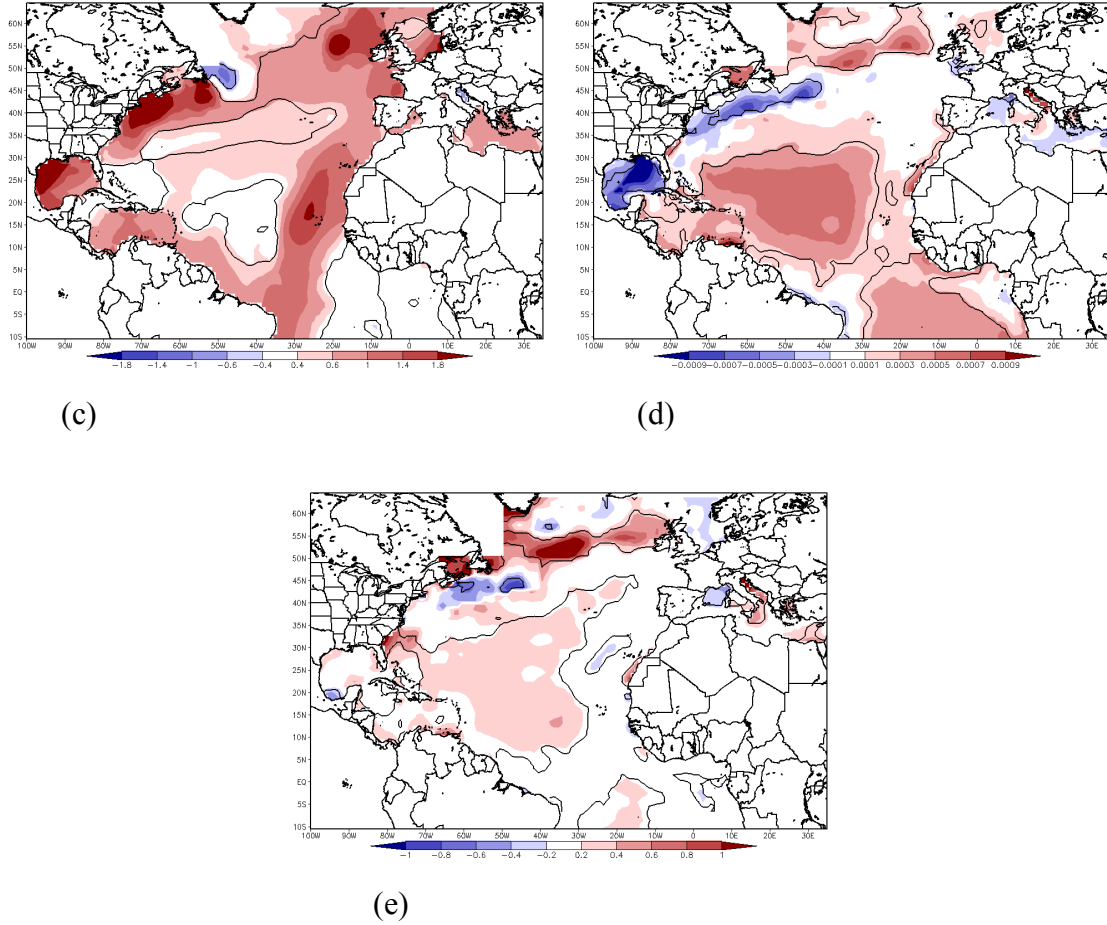


Figure 4. —continued

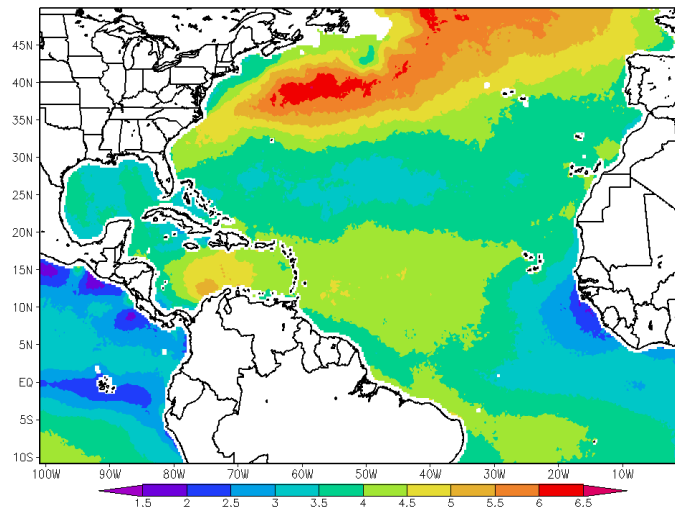
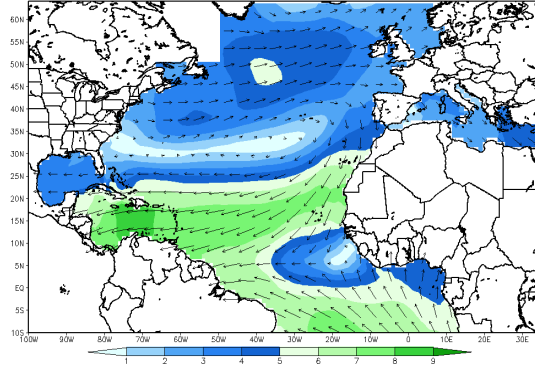
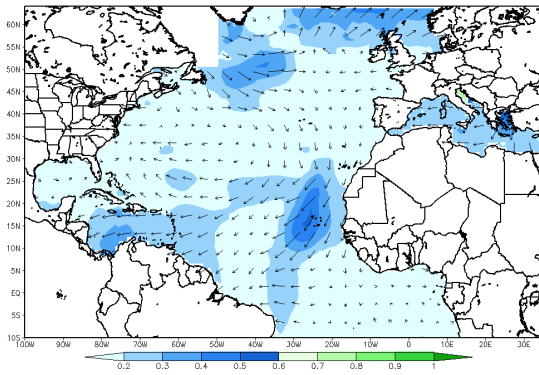


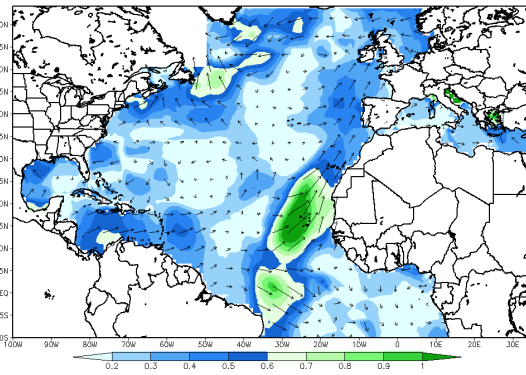
Figure 5. Comparison of pre and post 1998 wind speeds (ms^{-1}) using the Special Sensor Microwave/Imager (SSM/I) derived monthly fields. 1993-1997 overall mean minus 1998-2003.



(a)



(b)



(c)

Figure 6. Comparison of the vector winds during 1982-1997 and 1982-2003 to the 1978-2003 climatology. (a) 1978-2003 climatology (ms^{-1}). (b) Vector wind anomalies for 1982-1997 (ms^{-1}). (c) Vector wind anomalies for 1998-2003 (ms^{-1}).

CHAPTER 6

SUMMARY

The spatial and temporal variability of the surface turbulent heat fluxes over the North Atlantic was examined using the new objectively produced FSU3 gridded wind and surface flux product for 1978-2003. The FSU3 product is derived from in situ ship and buoy observations using a variational method. A cost function based on weighted constraints is minimized in the process of determining the surface fluxes.

The analysis shows that the surface turbulent heat fluxes exhibit a low frequency (basin wide) mode of variability over the North Atlantic where the latent and sensible heat flux anomalies transition from predominantly positive to negative values around 1998. The timing of the transition along with the basin wide extent of the signal indicates a possible link to the AMO. The variation in the latent and sensible heat fluxes is forced by changes in the large scale circulation patterns, with the wind speed acting as the primary forcing mechanism.

Zonal averages show a clear distinction between the heat fluxes and wind speed during 1982-1997 and 1998-2003 over the region extending from the equator to roughly 40°N, with the former time period having larger values. The humidity and air/sea temperature differences show much less dissimilarity between the two time periods. The largest differences between the two time periods for the latent heat fluxes occur over the tropical, Gulf Stream, and higher latitude regions of the North Atlantic. The largest sensible heat flux differences are limited to regions along the New England coast and poleward of 40°N; however values over the tropics and central North Atlantic are statistically significant. The location of the greatest wind speed differences (periphery of the subtropical high) suggests a change in the meridional pressure gradient. Vector anomalies show a weakening of the large scale circulation patterns during 1998-2003.

The similarities between the pre 1982 and post 1998 values demonstrates the need to extend the time series back in time to further capture the interdecadal variability. It appears that the data density in the Atlantic basin is sufficient to at least double the length of the time series.

REFERENCES

- Alexander, M. A. and J. D. Scott, 1997: Surface Flux Variability over the North Pacific and North Atlantic Oceans. *J. Climate*, **10**, 2963-2978.
- Berry, D. I., E. C. Kent, and P. K. Taylor, 2004: An Analytical Model of Heating Errors in Marine Air Temperature for Ships. *J. Atmos. Oceanic Technol.*, **21**, 1198-1215.
- Bourassa, M. A., D. G. Vincent, and W. L. Wood, 1999: A Flux Parameterization Including the Effects of Capillary Waves and Sea State. *Journal of the Atmospheric Sciences*, **56**, 1123-1139.
- , M. A., R. Romero, S. R. Smith, and J. J. O'Brien, 2005: A New FSU Winds Climatology. *J. Climate*, **18**, 3686-3698.
- Cayan, D. R., 1992: Latent Heat Flux Anomalies over the Northern Oceans: The Connection to Monthly Atmospheric Circulation. *J. Climate*, **5**, 354-369.
- Curtis, S. and S. Hastenrath, 1995: Forcing of Anomalous Sea Surface Temperature Evolution in the Tropical Atlantic during Pacific Warm Events. *J. Geophys. Res.*, **100**, 15835-15847.
- da Silva, A., A. C. Young, and S. Levitus, 1994: *Algorithms and Procedures*. Vol. 1, *Atlas of Surface Marine Data 1994*, NOAA Atlas NESDIS 6, 83 pp.
- Delworth, T. L. and M. E. Mann, 2000: Observed and Simulated Multidecadal Variability in the Northern Hemisphere. *Clim. Dyn.*, **16**, 661-676.
- Deser, C., J. E. Walsh, and M. S. Timlin, 2000: Arctic Sea Ice Variability in the Context of Recent Atmospheric Circulation Trends. *J. Climate*, **13**, 617-633.
- Donlon, C. J. and I. S. Robinson, 1997: Observations of the Oceanic Thermal Skin in the Atlantic Ocean. *J. Geophys. Res.*, **102**, 18585-18606.
- Enfield, D. B., A. M. Mestas-Nunez, and P. J. Trimble, 2001: The Atlantic Multidecadal Oscillation and its Relation to Rainfall and River Flows in the Continental U.S.. *Geophys. Res. Lett.*, **28**, 2077-2080.

- Giannini, A., J. C. H. Chiang, M. A. Cane, Y. Kushnir, and R. Seager, 2001: The ENSO Teleconnection to the Tropical Atlantic Ocean: Contributions of the Remote and Local SSTs to Rainfall Variability in the Tropical Americas. *J. Climate*, **14**, 4530-4544.
- Goldenberg, S. B., C. W. Landsea, A. M. Mestas-Nunez, and W. M. Gray, 2001: The Recent Increases in Atlantic Hurricane Activity: Causes and Implications. *Science*, **293**, 474-479.
- Gray, S. T., L. J. Graumlich, J. L. Betancourt, and G. T. Pederson, 2004: A Tree-ring Based Reconstruction of the Atlantic Multidecadal Oscillation Since 1567 A.D.. *Geophys. Res. Lett.*, **31**, L12205-L12205.
- Hurrell, J. W., 1995: Decadal Trends in the North Atlantic Oscillation: Regional Temperatures and Precipitation. *Science*, **269**, 676-679.
- , and H. van Loon, 1997: Decadal Variations associated with the North Atlantic Oscillation. *Climatic Change*: Vol. 36, pp.301-326.
- , and R.R. Dickson, 2004: Climate variability over the North Atlantic. Marine Ecosystems and Climate Variation - the North Atlantic. N.C. Stenseth, G. Ottersen, J.W. Hurrell, and A. Belgrano, Eds. Oxford University Press, 2004.
- Kalnay, E., and Coauthors, 1996: The NCEP/NCAR 40-Year Reanalysis Project. *Bull. Amer. Meteor. Soc.*, **77**, 437-471.
- Kara, A. B., A. J. Wallcraft, and H. E. Hurlburt, 2006: Land contamination of atmospheric forcing for ocean models near land-sea boundaries. *J. Phys. Oceanogr.*, in press.
- Kerr, R. A., 2000: A North Atlantic Climate Pacemaker for the Centuries. *Science*, 1984-1985.
- Lamb, P. J. and R. A. Pepler, 1987: North Atlantic Oscillation: Concept and an Application. *Bull. Amer. Meteor. Soc.*, **68**, 1218-1225.
- Lindau, R., 1995: A new Beaufort equivalent scale. *Proc. Int. COADS Winds Workshop*, Kiel, Germany, Institut für Meereskunde Kiel and NOAA, 232-252
- NCDC, 2003: Data documentation for Data Set 1129: Marine data. Tech. Doc. TD-1129, 31 pp. [Available from NCDC, 151 Patton Ave., Asheville, NC 28801-5001.].
- Pegion, P. J., M. A. Bourassa, D. M. Legler, and J. J. O'Brien, 2000: Objectively Derived Daily "Winds" from Satellite Scatterometer Data. *Mon. Wea. Rev.*, **128**, 3150-3168.
- Philander, S. G., 1990: El Nino, La Nina, and the Southern Oscillation. Academic Press.

- Reynolds, R. W., 1988: A Real-Time Global Sea Surface Temperature Analysis. *J. Climate*, **1**, 75-86.
- Rogers, J. C., 1990: Patterns of Low Frequency Monthly Sea Level Pressure Variability (1899-1986) and Associated Wave Cyclone Frequency. *J. Climate*, **3**, 1364-1379.
- , 1997: North Atlantic Storm Track Variability and Its Association to the North Atlantic Oscillation and Climate Variability of Northern Europe. *J. Climate*, **10**, 1635-1647.
- Schlesinger, M. E. and N. Ramankutty, 1994: An Oscillation in the Global Climate System of Period 65-70 Years. *Nature*, **367**, 723-726.
- Serreze, M. C., F. Carse, R. G. Barry, and J. C. Rogers, 1997: Icelandic Low Cyclone Activity: Climatological Features, Linkages with the NAO, and Relationships with Recent Changes in the Northern Hemisphere Circulation. *J. Climate*, **10**, 453-464.
- Shanno, D. F., and K. H. Phua, 1980: Remark on Algorithm 500- A Variable Method Subroutine for Unconstrained Nonlinear Minimization. *ACM Trans. Math. Software*, **6**, 618-622.
- Sutton, R. T. and D. L. R. Hodson, 2005: Atlantic Ocean Forcing of North American and European Summer Climate. *Science*, **309**, 115-118.
- Taylor, P. K., and WCRP/SCOR Working Group on Air-Sea Fluxes, 2000: Intercomparison and Validation of Ocean-Atmosphere Energy Flux Fields (November 2000). WMO/TD No. 1036, 306 pp.
- van Loon, H. and J. C. Rogers, 1978: The Seesaw in Winter Temperatures between Greenland and Northern Europe. Part I: General Description. *Mon. Wea. Rev.*, **106**, 296-310.
- Wahba, G., and J. Wendelberger, 1980: Some New Mathematical Methods for Variational Objective Analysis Using Splines and Cross-Validation. *Mon. Wea. Rev.*, **108**, 1122-1143.
- Walker, G. T., and E. W. Bliss, 1932: World Weather V. *Mem. Roy. Meteor. Soc.*, **4**, 53-84.
- Woodruff, S. D., R. J. Slutz, R. L. Jenne, and P. M. Steurer, 1987: A Comprehensive Ocean-Atmosphere Data Set. *Bull. Amer. Meteor. Soc.*, **68**, 1239-1250.
- , S. D., H. F. Diaz, J. D. Elms, and S. J. Worley, 1998: COADS Release 2 Data and Metadata Enhancements for Improvements of Marine Surface Flux Fields. *Phys. Chem. Earth*, **23**, 517-526.
- Worley, S. J., S. D. Woodruff, R. W. Reynolds, S. J. Lubker, and N. Lott, 2005: ICOADS Release 2.1 Data and Products. *Int. J. Climatol.*, **25**, 823-842.

Zhao, Y. P., and G. A. McBean, 1986: Annual and Interannual Variability of the North Pacific Ocean-to-Atmosphere Total Heat Transfer. *Atmosphere-Ocean*, **24**, 265-282.

BIOGRAPHICAL SKETCH

I was born on January 6, 1981 and raised in Mountain Top, Pennsylvania. In the spring of 2003, I graduated from Millersville University with a B.S. in Meteorology. In the fall of 2003, I came to Florida State University to pursue a M.S. in Meteorology.